ACCEPTANCE CALCULATION AND STUDY OF FAULT SCENARIOS IN THE PIP-II LINAC*

R. Prakash[†#], A. Saini, S. Chandrasekaran, Fermilab, Batavia, IL 60510, U.S.A.
[†] Also at RRCAT, Indore, MP, India and HBNI, Mumbai.

Abstract

The Proton Improvement Plan (PIP)-II is a proposed high intensity proton facility being developed at the Fermilab. The PIP-II is primarily based on construction of a new superconducting radio frequency (SRF) linear accelerator (linac) that would deliver an average beam current of 2mA with output energy up to 800 MeV. The acceptance of an accelerator outlines its sensitivity against deviations from its nominal design parameters. Consequently, a higher acceptance minimizes possibility of the beam loss. This paper presents longitudinal and transverse acceptance of the PIP-II SRF linac. Furthermore, paper also discusses implications of fault scenarios, such as the cavity failure, on the beam optics and acceptances.

INTRODUCTION

'Proton Improvement Plan (PIP)-II' is second stage of upgrades being planned to perform at existing accelerator complex at Fermilab. PIP-II is devised to enable the Fermilab accelerator complex to deliver a beam power in excess of mega-watt (MW) on target at the initiation of Long Baseline Neutrino Facility [1]. This in turn, requires construction of a new Continuous Wave (CW)-compatible SRF linac. PIP-II SRF linac will deliver H^- ions beam with a final kinetic energy of 800 MeV and an average current of 2 mA endowed with a special and flexible time structure to satisfy diverse experimental needs. A detailed description of the PIP-II linac was presented elsewhere [2].

SRF LINAC ARCHITECTURE

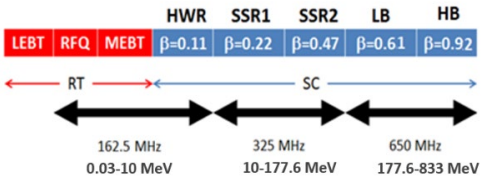

Figure 1: Acceleration scheme in the PIP-II linac. Red-coloured sections operate at room temperature while blue-coloured sections operate at 2K.

A schematic of the linac's architecture is shown in figure 1. It is composed of a warm front-end and an SRF accelerating section. The warm front-end consists of an ion source, a Low Energy Beam Transport (LEBT) line, an RFQ and, a Medium Energy Beam Transport line. Most of the beam manipulations happen in this part of the linac. The beam acceleration occurs mainly in the SRF linac. It is segmented into five sections i.e. Half Wave Resonator (HWR), Single Spoke Resonator (SSR) 1 & 2, Low Beta (LB) and High Beta (HB). Number of cryomodules (CM) and their configurations in each section are summarized in Table 1. Note that superconducting solenoids are used in HWR, SSR1 and SSR2 sections while warm quadrupole doublets are utilized in LB and HB sections.

Table 1: Numbers of elements and energy range in each section of the PIP-II SRF linac.

Section	CM	Cav/Mag per CM	Energy (MeV)
HWR	1	8/8	2.1-10
SSR1	2	8/4	10-32
SSR2	7	5/3	32-177
LB	9	4/1*	177-516
HB	4	6/1*	516-833

* one warm quadrupole doublet located between cryomodules in LB and HB sections

Stringent beam loss criterion of 1W/m used in the ion linac demands a higher acceptance of the linac. Focussing period changes regularly along the linac at the transition between two different section. As a result, the overall acceptance of the linac can shrink severely at each such transition if optics is not designed properly. In this paper, we have evaluated the acceptance in transverse and longitudinal plane for the PIP-II linac. Along the linac, the bottleneck locations for acceptance were also determined.

ACCEPTANCE CALCULATION FOR PIP-II SRF LINAC

The maximum size of the beam which can be transported through the linac without beam loss can be represented as acceptance of the linac [3]. Numerical simulation for acceptance calculation was done using beam dynamics code TraceWin [4]. Calculations were done in both the planes transverse and longitudinal. Simulations were carried out with large number of initial particles $7x10^5$. To estimate longitudinal acceptance, initial longitudinal emittance was set very high in comparison with the nominal emittance. Transverse emittance was kept at minimum to avoid any loss in the transverse plane. For transverse acceptance calculation, vice versa was done. To obtain the results, particle which

* This manuscript has been authored by Fermi Research Alliance, LLC under Contract No. DE-AC02-07CH11359 with the U.S. Department of Energy, Office of Science, Office of High Energy Physics.

survived at the linac end were identified. Particle distribution at linac entrance was plotted on a phase space and surviving particles were highlighted with a different color to show the acceptance area. The following initial parameters were used for the calculations –

Table 2: Initial parameters used in TraceWin for acceptance calculation.

Parameters	Acceptance Calculation		Nominal Values
	Long.	Trans.	
$\epsilon_x\ (\pi\ \mathrm{mm-mrad})$	10^{-4}	110	0.21
$\epsilon_y\ (\pi\ \mathrm{mm-mrad})$	10^{-4}	10^{-4}	0.21
$\epsilon_z\ (\pi\ \mathrm{deg-MeV})$	10	10^{-4}	0.064
$\beta_z\ (\mathrm{deg}/\pi-\mathrm{MeV})$	225.24	1.2	1.2
Current (mA)	0	0	5
Initial Particle	7×10^5	7×10^5	7×10^5
Distribution	Uniform	Uniform	6D Gaussian

LONGITUDINAL ACCEPTANCE

For the purpose of acceptance calculation, nominal optics without any alignment errors was used. A longitudinal phase space diagram $\Delta W\ vs\ \Delta\phi$ is plotted in Fig 2. Here ΔW and $\Delta\phi$ are the energy and phase width with respect to synchronous particle. The area represented by blue color is the input beam at the linac entrance. As described in Table 2, phase space of the input beam during acceptance calculation is kept bigger than the anticipated acceptance region. The green area inside the blue color region is known as acceptance region to the linac.

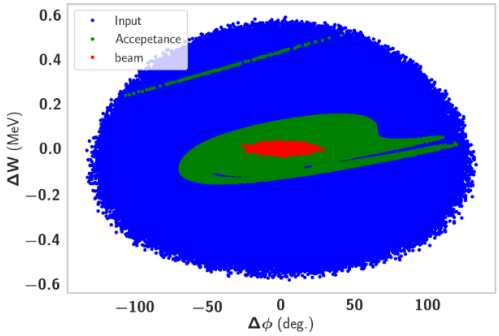

Figure 2: Longitudinal acceptance of the linac with $\Delta\phi$ at 162.5 MHz.

The phase space of the beam is plotted with red color. In order to transport the beam completely, it must be within the acceptance region (green area). Any particle which is outside the green region gets lost at some location along the linac. The green region exhibits typical golf club type of phase space which is the case of the accelerating beams. Figure 3 shows beam loss distribution along the linac while transporting the artificial beam. The minimum loss occurs in the HWR section (~0.02%) while maximum loss happens in the SSR1 section (~82.8%). A significant amount ~14.3% of the beam is also lost in SSR2 section. Very small (~1.5%) beam is lost in LB650 and HB650 sections.

Discontinuity in the average longitudinal focussing strength along the linac leads to large reduction of acceptance [5]. In order to determine the locations which cause maximum shrinkage in the acceptance of linac, the acceptance calculations were performed for different lengths of linac.

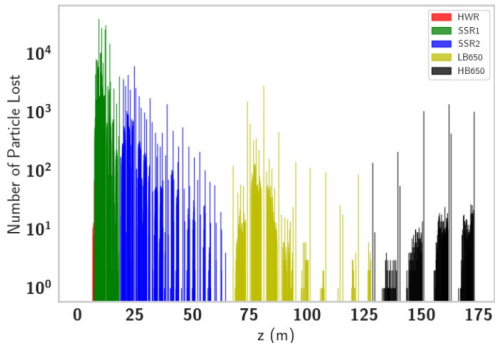

Figure 3: Particle loss along the linac.

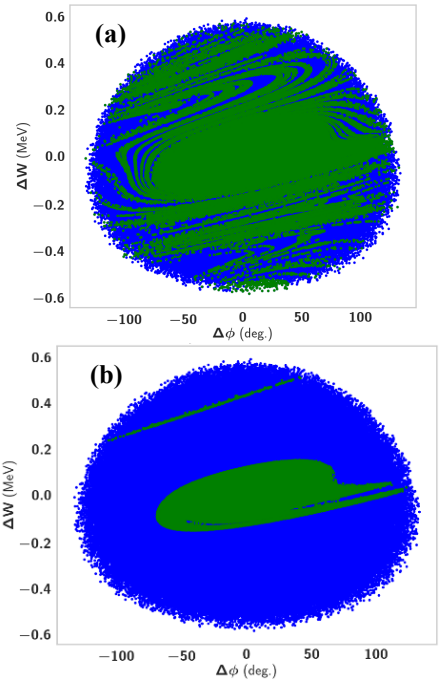

Figure 4: Acceptance Evolution through the linac, (a) HWR+SSR1 Section (b) HWR+SSR1 +SSR2 Section

The evolution of acceptance region is shown in the Fig 4. Figure 4(a) shows the acceptance of linac when HWR and SSR1 sections are is present. It should be noted here that acceptance of the linac shrinks rapidly due to SSR1 section. This inference is also validated by the Fig 3,

where SSR1 section shows maximum beam loss. When the linac is modified again to include SSR2 section along with HWR and SSR1, the acceptance region shrinks further more as shown in the Fig 4(b). Further, when LB650 and HB650 sections are included in calculation domain, they have very small effect on the acceptance area.

Effect of Cavity Failure on the Acceptance

Failure of RF cavity in the linac creates a beam mismatch with subsequent beam transport line. This results into reduction and smearing of the acceptance region. To investigate the effect of cavity failure on the longitudinal acceptance, 1st cavity of the HWR section was turned off. The resulting acceptance was plotted in Fig. 5. It should be noted that acceptance with cavity failure (yellow) has distorted shape in comparison to the acceptance without any failure (green). The beam still falls within the new acceptance area. Therefore, even after the cavity failure, no beam loss was observed for nominal baseline optics.

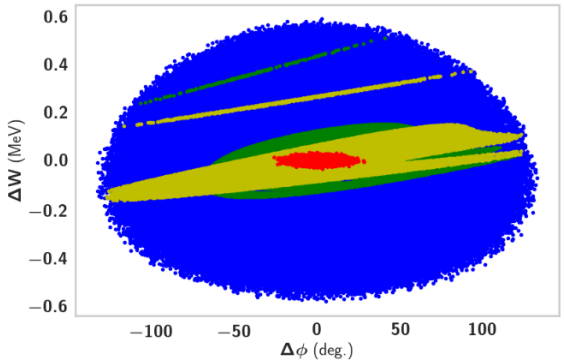

Figure 5: Longitudinal acceptance of the linac gets disturbed when first cavity of the HWR section is failed.

TRANSVERSE ACCEPTANCE

Transverse acceptance is evaluated with initial conditions described in Table 2. Transverse acceptance reflects the beam restrictions in the transverse plane. Transverse acceptance was calculated and plotted in Fig. 6. Here, like the previous plots, area with blue color represents the input beam to the linac and area with green and red colors represent acceptance and beam.

Effect of Solenoid Failure on the Transverse Acceptance

As discussed in the previous section, longitudinal acceptance gets disturbed due to cavity failure, in a similar way, transverse acceptance also gets changed due to the failure of focussing elements. To observe the effect of the focussing element failure on the transvers acceptance, the first solenoid was turned off, and effect was plotted in the Fig. 7. The new transverse acceptance is plotted in yellow and it is rotated in the plane compared with acceptance without any failure. It should be noted that beam still falls well within the new acceptance region.

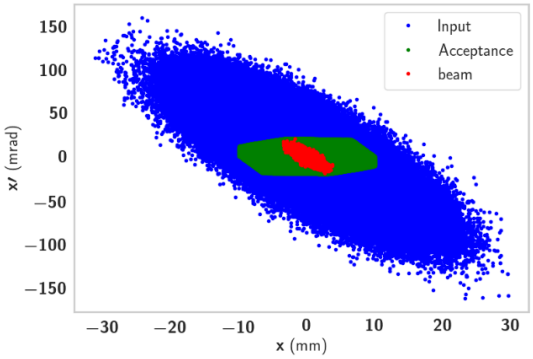

Figure 6: Transverse acceptance of the linac.

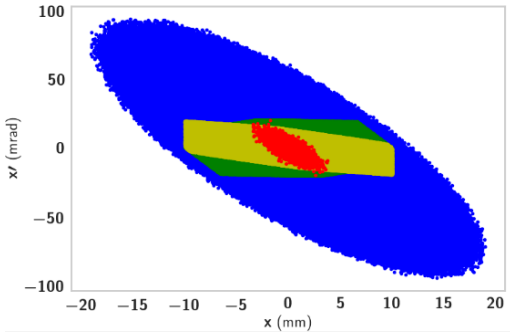

Figure 7: Effect of solenoid failure on the transverse acceptance. Nominal acceptance is shown in green and acceptance after 1st sol. failure is shown in yellow.

CONCLUSION

Longitudinal and transverse acceptance was calculated for the superconducting part of the PIP-II linac. It was confirmed that phase space area of the beam falls well within the acceptance region for both the cases - longitudinal and transverse. SSR1 and SSR2 are the most sensitive area of the linac where acceptance shrinkage happens. Failure of beamline element (cavity and solenoid) had adverse impact on the acceptance region. The acceptance was still sufficient to transport the beam.

ACKNOWLEDGEMENTS

Authors takes this opportunity to acknowledge entire PIP-II team and collaborators who are working in harmony for a successful realization of the project.

REFERENCES

[1] The DUNE Collaboration, “CDR Volume 1: The LBNF and DUNE Projects,” tech. rep., 2015.
[2] PIP-II Conceptual Design Report, 2017.
[3] Martin Reiser, “Theory and Design of Charged Particle” WILEY-VCH Verlag GmbH & Co. KGaA, Weinheim, 2008
[4] http://irfu.cea.fr/dacm/logiciels/
[5] A. Saini et al., “Calculation of Acceptance of High Energy Superconducting Proton Linac for Project-X”, in FERMILAB-CONF-11-123-APC.